Published in final edited form as:
Free Radic Biol Med. 2010 November 30; 49(10): 1574–1581. doi:10.1016/j.freeradbiomed.2010.08.019.

Ferricytochrome *c* Protects Mitochondrial Cytochrome *c* Oxidase Against Hydrogen Peroxide-Induced Oxidative Damage

Erik Sedlák[§], **Marian Fabian**[‖], **Neal C. Robinson**, and **Andrej Musatov**[*]
Department of Biochemistry, The University of Texas Health Science Center, San Antonio, TX 78229-3900, USA

Abstract

Excess of ferricytochrome *c* protects purified mitochondrial cytochrome *c* oxidase and bound cardiolipin from hydrogen peroxide-induced oxidative modification. All of the peroxide-induced changes within cytochrome *c* oxidase, such as oxidation of $Trp_{19,IV}$ and $Trp_{48,VIIc}$, partial dissociation of subunits VIa and VIIa, and generation of cardiolipin hydroperoxide, no longer take place in the presence of ferricytochrome *c*. Furthermore, ferricytochrome *c* suppresses the yield of H_2O_2-induced free radical detectable by electron paramagnetic resonance spectroscopy within cytochrome *c* oxidase. These protective effects are based on two mechanisms. The first involves the peroxidase/catalase-like activity of ferricytochrome *c*, which results in the decomposition of H_2O_2, with the apparent bimolecular rate constant of $5.1 \pm 1.0\ M^{-1}s^{-1}$. Although this value is lower than the rate constant of a specialized peroxidase, the activity is sufficient to eliminate H_2O_2-induced damage to cytochrome *c* oxidase in the presence of an excess of ferricytochrome *c*. The second mechanism involves ferricytochrome *c*-induced quenching of free radical(s) generated within cytochrome *c* oxidase. These results suggest that ferricytochrome *c* may have an important role in protection of cytochrome *c* oxidase and consequently the mitochondrion against oxidative damage.

Keywords

cytochrome *c* oxidase; cytochrome *c*; oxidative damage; peroxidase activity; free radicals; hydrogen peroxide

INTRODUCTION

The mitochondrion has a central role in the production of ATP as well as the generation of reactive oxygen species (ROS). Under physiological conditions, the mitochondrion converts ~1–2% of the consumed oxygen into superoxide anion [1]. Moreover, ROS concentrations increase significantly under certain pathological events such as ischemia-reperfusion [2], muscular dystrophy [3], atherosclerosis [4], Parkinson's disease [5], or other age-related disorders. Mitochondrial superoxide radicals are generated primarily by two ubiquinone utilizing electron transport complexes, i.e., Complex I (NADH:ubiquinone oxidoreductase), and Complex III (ubiquinone-cytochrome *c* reductase) [6,7]. Normally, the resulting

[*]Corresponding author. musatov@uthscsa.edu. Telephone: (210) 567-3779. Fax: (210) 567-6595.
[§]Permanent address: Department of Biochemistry, P. J. Šáfarik University, Moyzesova 11, 04167 Košice, Slovakia.
[‖]Department of Biochemistry and Cell Biology, Rice University, P.O. Box 1892, Houston, Texas 77251-1892, USA.

superoxide anion is converted to H_2O_2 by superoxide dismutase with subsequent conversion to H_2O by catalase or glutathione peroxidase. However, in the presence of transition metals, H_2O_2 is converted into highly reactive hydroxyl radicals. Because the electron transfer chain components are a major source of superoxide, the local concentration of ROS near the inner membrane is potentially quite high, making the electron transfer chain itself a potential target for oxidative damage. If the resulting damage inhibits one or more of the complexes, ROS production by complexes I and III would be expected to increase in a manner analogous to that caused by electron transport inhibitors. As a result, ROS damage to the electron transfer chain could initiate a cascade of structural and functional alterations within inner mitochondrial membrane, the entire mitochondrion, and other cell components. In order to survive such a ROS attack, the mitochondrial electron transfer complexes must be equipped with efficient protective mechanisms.

Cytochrome c oxidase (CcO, EC 1.9.3.1.) is one of the mitochondrial electron transfer complexes known to be inactivated by ROS [8,9,10,11,12]. This enzyme catalyzes the transfer of electrons from ferrocytochrome *c* to oxygen, a reaction that proceeds through two oxy-intermediates, “peroxy-” and “ferryl-CcO”, both of which are potential free radical sources [13,14,15]. During normal electron flux, the concentration of these transient intermediates is quite low; however, during the lifetime of the mitochondrion, the potential exists for chronic free radical exposure. To avoid damage to redox-active sites, CcO is equipped with several defense mechanisms. For example, subunit III of CcO has been proposed to protect CcO from oxidative damage during enzymatic turnover [8]. An amino acid aromatic network within CcO, that facilitates radical transfer away from the redox-active, binuclear center, may also protect the enzyme from damage by radicals generated near the active site [16,17].

Cytochrome *c* is located in the mitochondrial inter-membrane space where its main function is to shuttle electrons from cytochrome bc_1 to CcO during respiration. In addition to its function in mitochondrial respiration, cytochrome *c* has a significant role in activation of a programmed cell death cascade [18]. For example, dissociation of cytochrome *c* from the inner mitochondrial membrane is known to be a critical step in the initiation of apoptosis [19,20,21]. Cytochrome *c* can also function as a cardiolipin-specific oxygenase that chemically oxidizes cardiolipin to produce CL hydroperoxides [21]. The resulting oxidized CL then releases pro-apoptotic factors into the cytosol. In addition to these roles, cytochrome *c* is also known to alter both the generation and elimination of H_2O_2 [22,23,24], and to regenerate dioxygen from superoxide radical anion under conditions of oxidative stress [25].

In this study, we tested the hypothesis that CcO is protected from peroxide-induced oxidative damage by its natural mitochondrial partner, cytochrome *c*. This hypothesis is based upon the facts that: 1) cyt c^{3+} can destroy H_2O_2 [23,24]; and 2) cyt c^{3+} binding to CcO alters the conformation of the CcO catalytic binuclear center [26,27,28]. Therefore, we have examined the extent of H_2O_2-induced changes to purified, detergent-solubilized CcO in the presence and absence of excess ferricytochrome *c*.

EXPERIMENTAL PROCEDURES

Materials

Sodium cholate, hydrogen peroxide, horse heart cytochrome *c* (≥ 95% purity), ammonium iron sulfate hexahydrate, butylated hydroxytoluene, xylenol orange, and 2,2-diphenyl-1-picryl-hydrazyl (DPPH) free radical were purchased from Sigma-Aldrich Co. Dodecyl maltoside was from Anatrace Inc. Bovine cardiolipin was obtained from Avanti Polar Lipids. Triton X-100 was from Roche Diagnostics. Other chemicals were analytical grade.

Methods

Purification of Cytochrome c Oxidase from bovine heart—Two forms of purified CcO, designated as A and B, were used in the present work. Preparation A involves sodium cholate solubilization of sodium deoxycholate treated Keilin-Hartree heart muscle particles followed by purification of CcO by ammonium sulfate precipitation as previously described [29]. The resulting purified enzyme was dissolved at ~100 μM in pH 7.4 buffer containing 25 mM sodium cholate and stored at −60 °C. Before it was used, the enzyme was diluted to 5–10 μM with 2 mM dodecyl maltoside, pH 7.4 buffer followed by exhaustive dialysis at 4 °C against the same buffer to remove residual sodium cholate. Preparation B involves Triton X-100 solubilization of CcO from mitochondria at neutral pH followed by purification using ion-exchange chromatography in the presence of Triton X-100. Triton X-100 was replaced with dodecyl maltoside by the second ion exchange procedure [30,31]. The resulting enzyme was concentrated to ~200 μM in dodecyl maltoside containing buffer and stored at −60 °C. The first procedure produces a form of CcO that reacts slowly with heme a_3 binding ligands; the second procedure produces a form of CcO that reacts quickly with these same heme a_3 binding ligands [32]. The data presented in this work were obtained using five different preparations of CcO with essentially the same results. All assays were done at least in triplicate using at least two different enzyme preparations.

Reaction of Cytochrome c Oxidase with H_2O_2 in the Presence or Absence of Ferricytochrome c—Dodecyl maltoside-solubilized CcO, either preparation A or B, at 10 μM in 20 mM Tris-Cl containing 2 mM dodecyl maltoside was reacted with 500 μM H_2O_2 for 30 min at room temperature in the presence or absence 0–500 μM of cyt c^{3+}. In experiments that included cyt c^{3+}, H_2O_2 was added 5 min after cyt c^{3+} had been mixed with CcO. The reaction was stopped by removal of both H_2O_2 and cyt c^{3+} by HiTrap Q anion-exchange column chromatography [33]. This chromatographic procedure also removes almost all phospholipids bound to CcO, except for the 3–4 tightly bound cardiolipin [33]. The resulting CcO was subsequently analyzed for changes in activity, modification of subunits and peroxidation of bound cardiolipin. It made no difference in these experiments, whether oxidized cyt *c* was used directly as purchased, or fully oxidized by treatment with potassium ferricyanide followed by removal of potassium ferricyanide by dialysis for 15 hours at 4 °C. In either case, cyt c^{3+} concentration was determined using ε_{410nm} = 106.1 mM^{-1} cm^{-1} [34], while the concentration of H_2O_2 was calculated using ε_{240nm} = 40 $M^{-1}cm^{-1}$ [35]. The concentration of the “peroxy” and/or “ferryl” forms of CcO were determined from the difference spectra of H_2O_2-treated minus oxidized CcO using either $\Delta\Delta\varepsilon_{434\text{-}412nm}$ = 65 $mM^{-1}cm^{-1}$ [36] for the mixture of both forms, or $\Delta\Delta\varepsilon_{607–630}$ = 11 $mM^{-1}cm^{-1}$ for **P**-form, and $\Delta\Delta\varepsilon_{580–630}$ = 5.3 $mM^{-1}cm^{-1}$ for **F**-form [37]. Cyanide-inhibited cyt *c* was prepared by reacting of 500 μM cyt c^{3+} with 10 mM KCN for 1 hour at RT. The formation of the cyanide-cyt c^{3+} complex was confirmed by spectral changes at 695 nm. All visible spectra were collected using an SLM Aminco 3000 diode array spectrophotometer.

Determination of Cytochrome c Oxidase Activity—CcO activity was measured spectrophotometrically by following the pseudo-first order rate of oxidation of 25 μM ferrocytochrome *c* by 1.75 nM CcO at pH 7.0 in 25 mM phosphate buffer containing 2 mM dodecyl maltoside [33].

Subunit Analysis by High-Performance Liquid Chromatography—Quantitative RP-HPLC analysis of CcO subunit content was done using gradient elution from a Vydac C_{18} reverse-phase column (5 μm, 0.46 × 25 cm, 300-Å pore size) and a Waters/Millipore liquid chromatography system [9,16,38]. The gradient was made from mixtures of solvent A (0.2% TFA in water) and solvent B (0.2% TFA in acetonitrile). The column was equilibrated

with solvent A and subunits eluted at 1 mL/min with a linear gradient from 25 to 50 % solvent B in 50 min, followed by a linear gradient from 50 to 85 % solvent B in 17.5 min. Elution was monitored at 214 nm after loading 0.2 – 2.0 nmol of unmodified or H_2O_2-modified CcO. Percent yield of each subunit was based upon quantitative integration of peak areas as compared with unmodified, purified CcO [9,16,38]. Fractions (0.5 mL) were collected for analysis of unmodified and modified subunits by mass spectrometry.

Analysis of Cardiolipin Oxidation—The extent of conjugated diene generation within cardiolipin after exposure of CcO to H_2O_2 was determined spectrally after (Bligh and Dyer) extraction of all phospholipids from CcO using chloroform/methanol/water [39] and subsequent purification of cardiolipin by normal phase HPLC [40]. Conjugated diene formation was monitored by the increase in absorbance at 234 nm [41].

Mass Spectrometry—Matrix-assisted laser desorption ionization time-of-flight (MALDI-TOF) mass spectra were acquired on an Applied Biosystems Voyager-DE-STR operated in either the linear or reflectron mode. HPLC-electrospray ionization tandem mass spectra were obtained using a Finnigan LCQ in conjunction with a Michrom BioResources MAGIC 2002 micro HPLC connected to a home-built microspray interface. Mass spectrometry analysis of modified and unmodified CcO subunits was done as described previously [9,16,17].

EPR Spectroscopy—EPR spectra were recorded with a Varian E-6 spectrometer. Acquisition conditions of the spectra were: modulation amplitude 10 G, frequency 9.225 GHz, microwave power 200 μW and temperature 109 K. Two series of H_2O_2-treated samples were analyzed by EPR spectroscopy to determine the effect of cyt c^{3+} upon H_2O_2-induced radical generation within CcO. The first was a mixture of CcO and a variable amount of ferricytochrome *c*; the second was only cyt c^{3+}. In CcO-containing samples, 50 μM CcO, solubilized in 1 mM dodecyl maltoside pH 7.4 buffer containing 20 mM Tris-Cl and 4 mM K_2SO_4, was incubated with ferricytochrome *c* at room temperature (RT) for 5 minutes, followed by the addition of 300 μM H_2O_2. After 10 sec, the samples were rapidly frozen by immersion in a methanol-dry ice bath and then transferred into liquid nitrogen. Time-dependence of the radical signal was obtained by warming the samples to room temperature. After incubation of certain time the samples were frozen and used for EPR measurement. The concentration of radical within CcO was determined by the double integration of the EPR signal and comparison of the resulting area with that of DPPH standard. DPPH was solubilized in dimethyl sulfoxide and concentration calculated from the absorbance spectrum using an extinction coefficient of $\varepsilon_{525nm} = 11.9\ mM^{-1}cm^{-1}$ [42].

Rate of H_2O_2 Decomposition by Ferricytochrome c and Cytochrome c Oxidase —The H_2O_2 concentration was measured at discrete time intervals after mixing with either cyt c^{3+}, CcO or mixture of both proteins using the ferrous ion oxidation-xylenol orange assay (FOX2) [43]. The reaction conditions were 20 mM Tris-Cl buffer at pH 7.4, 2 mM dodecyl maltoside and 500 μM H_2O_2 mixed with either: 1) 500 μM cyt c^{3+}; 2) 10 μM CcO; or 3) the mixture of 500 μM cyt c^{3+} and 10 μM CcO. Each reaction was initiated by the addition of H_2O_2, stopped at 5 min intervals by removal of H_2O_2 using a Microcon, Ultracel YM-3 membrane filter, with 3000 Da cutoff. Peroxide concentration in the filtrate was determined by absorbance at 560 nm 30 min after addition of the FOX2 reagent (1/9 v/v) using a standard calibration curve.

RESULTS

Ferricytochrome c Prevents H_2O_2-induced Oxidative Damage to CcO

The reaction of H_2O_2 with detergent-solubilized CcO is known to cause a time- and concentration-dependent inactivation of the enzyme [16]. The electron-transport activity of H_2O_2-treated CcO decreases 50–80% after reaction with 500 μM H_2O_2 for 30 min. at RT (inset to Figure 1). However, significant protection from H_2O_2-induced inactivation occurs when at least a 20-fold molar excess of cyt c^{3+} is added to the reaction mixture, e.g., only 5 % inactivation occurs if 200 μM cyt c^{3+} is present (Figure 1). Excess cyt c^{3+} also prevents two other H_2O_2-induced effects: 1) oxidation of $Trp_{48,IV}$ and $Trp_{19,VIIc}$ and 2) partial dissociation of subunits VIa and VIIa (Figures 2 & 3). When excess cyt c^{3+} is not included, ~20% of IV ~50% of VIIc elute with altered elution times due to oxidation of a single tryptophan ($Trp_{48,IV}$ and $Trp_{19,VIIc}$) within each subunit [16]. The RP-HPLC elution peaks corresponding to the two oxidized subunits are absent if excess cyt c^{3+} is present during H_2O_2 exposure, i.e., > 90% of VIIc and nearly 100% of subunit IV remain unmodified (Figure 2 & 3). H_2O_2-induced oxidation of $Trp_{48,IV}$ and $Trp_{19,VIIc}$ without cyt c^{3+} and the absence of tryptophan oxidation in presence of cyt c^{3+} was also monitored by mass spectrometry as described previously [16,17]. In addition, excess cyt c^{3+} prevents dissociation of subunits VIIa and VIa, which normally accompanies H_2O_2-induced oxidative damage to CcO [16]. Only ~15% of subunit VIIa dissociates from CcO when it is exposed to H_2O_2 in the presence of at least a 20-fold molar excess of cyt c^{3+}, rather than >40% dissociation of this subunit in its absence. Dissociation of subunit VIa is considerably reduced as well (Figure 3, panel B).

Ferricytochrome c Protects Cardiolipin from Hydrogen Peroxide-Induced Peroxidation

Inclusion of cyt c^{3+} also protects cardiolipin that is bound to CcO from H_2O_2-induced peroxidation. If either pure or protein-bound cardiolipin is exposed to peroxides, a significant portion of the non-conjugated double bonds is converted into conjugated dienes with characteristic absorbance at 234 nm (Figure 4, thick line). However, if CcO is exposed to high concentrations of H_2O_2 in the presence of excess cyt c^{3+}, the double bonds are well protected from oxidation as evident from the significantly reduced absorbance at 234 nm (Figure 4, dashed line).

Hydrogen Peroxide-induced Spectral Changes for Cytochrome c Oxidase and Ferricytochrome c

Reaction of H_2O_2 with CcO results in the formation of two oxy-intermediates, the “peroxy-” or **P**-form” and the “ferryl-” or **F**-form, both of which are detected by visible spectroscopy [36]. Inclusion of cyt c^{3+} does not alter either the relative amounts or rates at which the two intermediates are generated. Reaction of 1.2 μM CcO with 500 μM H_2O_2, either in the presence or absence of 8 μM cyt c^{3+}, produces a mixture that contains 0.36–0.48 μM **P**-form, and 0.68–0.76 μM **F**-form, i.e., 35 – 40% and 60%–65%, respectively (Figure 5). The pseudo-first order rate constants for the formation of the oxy-intermediates are also nearly identical in the presence or the absence of 100 μM cyt c^{3+} i.e., 0.041 s^{-1} and 0.039 s^{-1}, respectively (data not shown).

Hydrogen peroxide also reacts with cyt c^{3+}, but the spectral effects are minimal under the conditions used. For example, maximum absorbance in the Soret region decreases by <5% when 500 μM cyt c^{3+} is exposed to 500 μM of H_2O_2 for 30 min (Figure 6, main panel). Such exposure slightly perturbs the charge-transfer bond between the heme iron and Met_{80} sulfur [44] since very small absorbance changes also occur at 695 nm (Figure 6, inset). However, H_2O_2 does not induce any major structural changes in cyt c^{3+} as evidenced by the

very small changes in the molar ellipticity at 417 nm (3–5%) and no significant alteration in either the far-UV or aromatic regions of the spectrum (data not shown).

H_2O_2-Induced Free Radical Generation within Cytochrome c Oxidase: Effect of Ferricytochrome c

Exposure of CcO to H_2O_2 generates a free radical EPR signal that is characterized by the g = 2.006 with a peak-to-trough width of 12 G (Figure 7, panel A). At 109 K this signal is saturated at a microwave power above 4 mW and no hyperfine structure is detected using amplitude modulation smaller than 10 G. A maximum yield of radical occurs 10 sec after addition of H_2O_2 and corresponds to ~14% of the CcO population. Inclusion of cyt c^{3+} suppresses the radical signal in a concentration- and time-dependent manner (Figure 7, panel B). This free radical is generated as H_2O_2 reacts with the catalytic binuclear center of CcO since the EPR signal is missing if the samples containing only ferricytochrome *c* and hydrogen peroxide, or if the catalytic site of CcO is first blocked with cyanide.

Decomposition of Hydrogen Peroxide by Ferricytochrome c and Cytochrome c Oxidase

Cyt c^{3+} exhibits peroxidase/catalase-type activity, which would be expected to decrease the H_2O_2 concentration [24,58]. To determine if this activity is sufficient to affect oxidative damage to CcO, the peroxidase/catalase-like activities of cyt c^{3+}, CcO, and a mixture of both proteins were determined by monitoring the catalytic destruction of H_2O_2. Both proteins catalyze a single exponential decrease in the H_2O_2 concentration with time (Figure 8). The activity of CcO is more than ten-times greater than cyt c^{3+}, with corresponding second order rate constants of 63.2 ± 2.5 $M^{-1}s^{-1}$ compared to a rate of 5.1 ± 1.0 $M^{-1}s^{-1}$ for cyt c^{3+}. Using these values, a pseudo-first order rate of (3.2 ± 0.6) $\times 10^{-3}$ s^{-1} is predicted for a mixture of 10 μM CcO and 500 μM cyt c^{3+}, which is within experimental error of the value experimentally determined, i.e., (3.8 ± 0.7) × 10^{-3} s^{-1}. The peroxidase/catalase-like activities of cyt c^{3+} and CcO are, however, completely inhibited if proteins are first reacted with cyanide (Figure 8). Presumably, cyanide reacts with a five-ligand form of cyt c^{3+} to produce a cyano – Fe^{3+} complex, which prevents subsequent reaction of the iron with H_2O_2.

DISCUSSION

H_2O_2-induced modifications to CcO are largely prevented by high concentrations of cyt c^{3+}. In contrast to results obtained in the absence of cyt c^{3+}, exposure of CcO to H_2O_2 in the presence of excess cyt c^{3+} leaves the electron-transport activity of CcO unaffected. Additionally, $Trp_{19,VIIc}$ and $Trp_{48,IV}$ both remain unmodified; dissociation of subunit VIIa is significantly reduced; peroxidation of cardiolipin is prevented; and the observed free radical concentration within CcO is reduced. The only H_2O_2-induced alteration not prevented by excess cyt c^{3+} is the dissociation of subunit VIa, which still occurs up to ~30%. The protective effects of cyt c^{3+} against time- and concentration-dependent H_2O_2-induced modification of CcO are the consequence of two quite different effects: (1) *c*yt c^{3+} catalyzed decomposition of H_2O_2, and (2) *c*yt c^{3+}-induced quenching of a peroxide-induced free radical within CcO.

Cyt c^{3+} catalyzed decomposition of H_2O_2

The mechanism for cyt c^{3+} catalyzed decomposition of H_2O_2 appears similar to either that of a classical peroxidase or catalase. Such activity would seem to be unlikely since cytochrome *c* contains six coordinate iron structure. However, the Met_{80} ligand bond is relatively weak and can be displaced by rather mild perturbants, e.g., changes in ionic strength or pH, allowing external ligands, such as cyanide, azide, imidazole and peroxide, to bind to the iron of cyt c^{3+} [24,45,46,47,48,49,50,51]. A small portion of cyt c^{3+} must be present in an “open” conformation in which the 6^{th} axial coordination bond with Met_{80} is

broken [52] to permit such binding. Since equilibrium between the "closed" and "open" cyt c^{3+} favors the "closed" 6-coordinate heme species H_2O_2 is expected to react slowly with cyt c^{3+}. Consistent with an "open" conformation hypothesis is the complete inhibition of peroxidase/catalase activity when cyt c^{3+} is first reacted with cyanide (Figure 8). Cyanide forms a strong coordination bond with any heme having an open 6^{th} ligand position; therefore, cyanide inhibition clearly demonstrates that catalytic destruction of H_2O_2 by cyt c^{3+} requires a direct interaction of H_2O_2 with the iron of cyt c^{3+}.

A peroxidase type mechanism raises the issue of an absence of reducing equivalents to complete the catalytic cycle. The small percentage of cyt c^{3+} in the "open" conformation would be expected to react with peroxide to form the typical peroxidase intermediate, compound I, containing ferryl oxygen, Fe(IV)═O, and a radical porphyrin cation, $R^{\bullet+}$. It is not obvious how the 2-electron reduction of compound I to regenerate cyt c^{3+} and water would occur, but a second H_2O_2 molecule may be the source of reducing equivalents, resulting in the disproportion of two peroxide molecules, i.e., a catalase-type reaction. Such a mechanism has been used to explain the H_2O_2-induced reduction of ferryl-oxygen compounds in both met-myoglobin [53,54] and cytochrome P450 [55]. Alternatively, the side chains of aromatic acids of protein itself may donate two electrons, i. e a peroxidase-type reaction.

Regardless of the mechanism for the peroxidase/catalase-like activity of cyt c^{3+}, there is no doubt that cyt c^{3+} catalyzes the slow decomposition of H_2O_2 with the second order rate of $5.1 \pm 1.0\ M^{-1}s^{-1}$ at pH 7.4. This rate is in good agreement with previously reported values of 4–11 $M^{-1}s^{-1}$ [56,57,58]. Although the peroxidase activity of cyt c^{3+} is ~6–7 orders of magnitude less than that of the 5-coordinate Fe structure in peroxidases, it is sufficient to significantly decrease the H_2O_2 concentration at high cyt c^{3+} concentration.

Cyt c^{3+}-Induced Quenching of a CcO free radical

The peroxidase/catalase activity of cyt c^{3+} satisfactorily explains a diminished effect of H_2O_2 on CcO due to partial destruction of H_2O_2, but it cannot explain the rapid decrease in the H_2O_2-induced free radical content of CcO. Inclusion of a 2–16 fold molar excess of cyt c^{3+} decreases the amount of the EPR-detectable radical by 30–45% 10 s after addition of peroxide. The slow peroxidase/catalase-like activity of cyt c^{3+} cannot appreciably alter the H_2O_2 concentration during such a short time interval (refer to Fig. 7).

The origin of the EPR-detectable free radical signal is unknown, but stoichiometric amounts of radicals are generated in proximity to the heme a_3-Cu_B site of CcO coincident with the formation of the peroxy- and ferryl-oxygen mixture. With both intermediates, the iron of heme a_3 is converted to an oxo-ferryl state with simultaneous generation of a radical cation, often assigned to Y_{244} (e.g. Fe_{a3}^{IV}═O Cu_B^{II} $Y_{244}^{\bullet+}$). The Y_{244} radical is not responsible for the EPR signal since electronic coupling of the radical to the iron and/or copper adjacent iron-copper binuclear center makes $Y_{244}^{\bullet+}$ EPR-silent. However, radical migration from Y_{244} to a site distant from the binuclear center would make it EPR visible and would explain the EPR signal. We previously postulated such radical migration away from Y_{244} along an "aromatic wire" to explain H_2O_2-induced oxidative damage to CcO-tryptophans located far from the binuclear center [16,17]. The yield of EPR detectable radical(s) in these distant site(s) is sub-stoichiometric with a maximum yield of only ~14%, but any radicals remaining near the binuclear center would go undetected. Alternatively, the steady state level of radicals may be less than stoichiometric because H_2O_2 acts as a 2-electron reductant to destroy the $Y_{244}^{\bullet+}$ radical cation before it can migrate away from the binuclear center (refer to prior discussion of peroxidase/catalase mechanism.

Three feasible mechanisms could explain the quenching of the EPR-detectable free radicals by cyt c^{3+}, but none of them is entirely satisfactory. First, cyt c^{3+} may form a complex with CcO that sufficiently alters the conformation of near the binuclear center [26,27,28] to suppress a radical migration away from the catalytic center (Y_{244}) to the secondary distant site(s). Consistent with this explanation is the decreased yield of the observed radical together with the inhibition of the modifications of the $Trp_{19,VIIc}$, $Trp_{48,IV}$ and cardiolipin in the presence of ferricytochrome *c*. This mechanism, however, is not completely acceptable since the cyt c^{3+}-induced CcO conformation would be expected to exhibit altered H_2O_2 reaction kinetics, which does not occur (generation of the oxy-intermediates and CcO peroxidase activity are nearly identical with, or without cyt c^{3+}; refer to Figures 5 & 7).

Second, cyt c^{3+} may participate in protein to protein free radical transfer in which case a protein of cyt c^{3+} would serve as an electron donor to a radical that had migrated to the surface of CcO, e.g., $Trp_{19,VIIc}$ or $Trp_{48,IV}$. We were unable to detect any such alterations to cyt c^{3+} although detection of such sub-stoichiometric amounts of radicals in a 20–50 fold excess of cyt *c* would be difficult.

Third, cyt c^{3+} could function as a shuttle of electrons to decrease free radical content. However, in absence of electron donors in our experimental conditions this mechanism is unlikely. Moreover, if such electron transfer is occurred it would have also affect the rate of formation of **P** and **F** intermediates during the reaction of oxidized enzyme with H_2O_2. Yet both the rates and amount of oxy-intermediates are the same in the presence and the absence of cytochrome *c* (Fig. 6).

We conclude that cyt c^{3+} assists in two ways to shield CcO against oxidative damage. First, cyt c^{3+} protects CcO by an external mechanism: catalytic removal of H_2O_2 by cyt c^{3+}. Although the rate of peroxidase activity of cyt c^{3+} is lower than for a specialized catalase or peroxidase, its location and high concentration in the mitochondrion (up to 0.7 mM [59]) potentially make cyt c^{3+} a significant contributor in the catalytic destruction of peroxide. Moreover, according to Kagan et al., interaction of cyt c^{3+} with mitochondrial cardiolipin significantly increases its peroxidase activity, which can become as high as ~200 $M^{-1}s^{-1}$ [21,60].

Second, cyt c^{3+} may also protect CcO from oxidative damage by suppression or elimination of detrimental free radical(s) that are generated as part of normal CcO turnover. In contrast to the purified enzyme, CcO within the mitochondrion is surrounded by cyt *c* on the matrix side of the inner membrane and, therefore, is well protected against H_2O_2-induced oxidative damage. In fact, CcO *in vivo* is relatively resistant to H_2O_2–induced oxidative damage. For example, with heterozygous Mn-superoxide dismutase knockout mice, mitochondrial H_2O_2 increases by 40–50% with significantly reduced complex I and complex V activities, but almost no detectable change in CcO electron-transport activity [61]. Furthermore, increasing the H_2O_2 concentration within isolated rat heart mitochondria, (i.e., conditions that are similar to those with knockout mice), does not lead to diminished CcO activity [62]. Purified CcO, however, is susceptible to hydrogen peroxide because it is separated from these defensive mechanisms. Altogether the present study suggests that cyt c^{3+} may have an important role in protecting the cytochrome oxidase and consequently mitochondrion as well against oxidative impairment.

Acknowledgments

This work was supported by grants from UTHSCSA (University Research Council grant for AM), National Institute of Health (NIH GM024795 for NCR and NIH GM0843348 for MF), and the Robert A. Welch Foundation (AQ1481 for NCR). Mass spectrometry data were acquired in the Institutional Mass Spectrometry Laboratory of the University of Texas Health Science Center at San Antonio. The authors thank Dr. Susan Weintraub for her

expert mass spectrometry analysis, Dr. Rastislav Varhač for invaluable discussions regarding these data, Ms. Tiffany McDonald-Marsh for excellent technical assistance and Dr. LeAnn K. Robinson for editorial help in preparing the manuscript.

ABBREVIATIONS

ROS	reactive oxygen species
CcO	bovine heart cytochrome *c* oxidase
P-and F-form	peroxy- and ferryl cytochrome *c* oxidase oxy-intermediates
cyt c^{3+}	ferricytochrome *c*
CL	cardiolipin (diphosphatidylglycerol)
DM	dodecyl maltoside
RT	room temperature
FOX2	ferrous ion oxidation-xylenol orange assay
HPLC	high-performance liquid chromatography
ESI/MS	electrospray ionization mass spectrometry
MALDI-TOF/MS	matrix-assisted laser desorption/ionization time-of-flight mass spectrometry
$Trp_{48,IV}$	tryptophan 48 within CcO subunit IV
$Trp_{19,VIIc}$	tryptophan 19 within CcO subunit VIIc

REFERENCES

1. Chance B, Williams GR. The respiratory chain and oxidative phosphorylation. Advances in Enzymol. 1956; 17:65–134.
2. Lesnefsky EJ, Hoppel CL. Ischemia-reperfusion injury in the aged heart: role of mitochondria. Arch. Biochem. Biophys. 2003; 420:287–297. [PubMed: 14654068]
3. Murphy ME, Kherer JP. Oxidation state of tissue thiol groups and content of protein carbonyl groups in chickens with inherited muscular dystrophy. Biochem. J. 1989; 260:359–364. [PubMed: 2764876]
4. Leeuwenburgh C, Rasmussen JE, Hsu FF, Mueller DM, Pennathur S, Heinecke JW. Mass spectrometric quantification of markers for protein oxidation by tyrosyl radical, cooper, and hydroxyl radical in low density lipoprotein isolated from human atherosclerotic plaques. J. Biol. Chem. 1997; 272:3520–3526. [PubMed: 9013599]
5. Cohen G. Oxidative stress, mitochondrial respiration, and Parkinson's disease. Ann. N.Y. Acad. Sci. 2000; 899:112–120. [PubMed: 10863533]
6. Turrens JF, Boveris A. Generation of superoxide anion by the NADH dehydrogenase of bovine heart mitochondria. Biochem. J. 1980; 191:421–427. [PubMed: 6263247]
7. Turrens JF, Alexandre A, Lehninger AL. Ubisemiquinone is the electron donor for superoxide formation by Complex III of heart mitochondria. Arch. Biochem. Biophys. 1985; 237:408–414. [PubMed: 2983613]
8. Bratton MR, Pressler MA, Hosler JP. Suicide inactivation of cytochrome c oxidase: catalytic turnover in the absence of subunit III alters the active site. Biochemistry. 1999; 38:16236–16245. [PubMed: 10587446]
9. Musatov A, Carroll CA, Liu Y-C, Henderson GI, Weintraub ST, Robinson NC. Identification of 4-Hydroxynonenal-Modified Subunits of Bovine Heart Cytochrome *c* Oxidase. Biochemistry. 2002; 41:8212–8220. [PubMed: 12069614]

10. Zhang Y, Marcillat O, Giulivi C, Ernster L, Davies KJA. The oxidative inactivation of mitochondrial electron transport chain components and ATPase. J. Biol. Chem. 1990; 265:16330–16336. [PubMed: 2168888]
11. Choksi KB, Nuss JE, Boylston WH, Rabek JP, Papaconstantinou J. Age-related increases in oxidatively damaged proteins of mouse kidney mitochondrial electron transport chain complexes. Free Radic. Biol. Med. 2007; 43:1423–1438. [PubMed: 17936188]
12. Chen J, Schenker S, Frosto TA, Henderson GI. Inhibition of cytochrome *c* oxidase activity by 4-hydroxynonenal (HNE). Biochim. Biophys. Acta. 1998; 1380:336–344. [PubMed: 9555085]
13. Ksenzenko, MYu; Vygodina, TV.; Berka, V.; Ruuge, EK.; Konstantinov, AA. Cytochrome oxidase-catalyzed superoxide generation from hydrogen peroxide. FEBS Lett. 1992; 297:63–66. [PubMed: 1312951]
14. Rich PR, Rigby SEJ, Heathcote P. Radicals associated with the catalytic intermediates of bovine cytochrome *c* oxidase. Biochim. Biophys. Acta. 2002; 1554:137–146. [PubMed: 12160986]
15. Wilson MT, Jensen P, Aasa R, Malmström PG, Vänngård T. An investigation by EPR and optical spectroscopy of cytochrome oxidase during turnover. Biochem. J. 1982; 203:483–492. [PubMed: 6288002]
16. Musatov A, Hebert E, Carroll CA, Weintraub ST, Robinson NC. Specific modification of two tryptophans within the nuclear-encoded subunits of bovine cytochrome c oxidase by hydrogen peroxide. Biochemistry. 2004; 43:1003–1009. [PubMed: 14744145]
17. Lemma-Gray P, Weintraub ST, Carroll CA, Musatov A, Robinson NC. Tryptophan 334 Oxidation in Bovine Cytochrome *c* Oxidase Subunit I Involves Free Radical Migration. FEBS Lett. 2007; 581:437–442. [PubMed: 17239857]
18. Liu X, Kim CN, Yang Y, Jemmerson R, Wang X. Induction of apoptotic program in cell-free extracts: requirement for dATP and cytochrome *c*. Cell. 1996; 86:147–157. [PubMed: 8689682]
19. Acehan D, Jiang X, Morgan DG, Heuser JE, Wang X, Akey CW. Three-dimensional structure of the apoptosome: implications for assembly, procaspase-9 binding, and activation. Mol. Cell. 2002; 9:423–432. [PubMed: 11864614]
20. Liu Z, Lin H, Ye S, Liu Q-Y, Meng Z, Zhang C-M, Xia Y, Margoliash E, Rao Z, Liu X-J. Remarkably high activities of testicular cytochrome c in destroying reactive oxygen species and in triggering apoptosis. Proc. Natl. Acad. Sci. 2006; 103:8965–8970. [PubMed: 16757556]
21. Kagan VE, Tyurin VA, Jiang J, Tyurina YY, Ritov VB, Amoscato AA, Osipov AN, Belikova NA, Kapralov AA, Kini V, Vlasova II, Zhao Q, Zou M, Di P, Svistunenko DA, Kurnikov IV, Borisenko GG. Cytochrome c acts as a cardiolipin oxygenase required for release proapoptotic factors. Nat. Chem. Biol. 2005; 1:223–232. [PubMed: 16408039]
22. Zhao Y, Wang Z-B, Xu J-X. Effect of cytochrome c on the generation and elimination of O2- and H_2O_2 in mitochondria. J. Biol. Chem. 2003; 278:2356–2360. [PubMed: 12435729]
23. Zhao Y, Xu JX. The operation of the alternative electron-leak pathways mediated by cytochrome *c* in mitochondria. Biochem. Biophys. Res. Commun. 2004; 317:980–987. [PubMed: 15094365]
24. Deterding LJ, Barr DP, Mason RP, Tomer KB. Characterization of cytochrome c free radical reactions with peptides by mass spectrometry. J. Biol. Chem. 1998; 273:12863–12869. [PubMed: 9582316]
25. Pereverzev MO, Vygodina TV, Konstantinov AA, Skulachev VP. Cytochrome *c*, an ideal antioxidant. Biochem. Soc. Trans. 2003; 31:1312–1315. [PubMed: 14641051]
26. Musatov A, Konstantinov AA. Conformational change of cytochrome a_3 induced by oxidized cytochrome *c*. FEBS Lett. 1988; 238:295–299. [PubMed: 2844603]
27. Hildebrandt P, Heimburg T, Marsh D, Powell GL. Conformational Changes in Cytochrome *c* and Cytochrome Oxidase upon Complex Formation: **A** Resonance Raman Study. Biochemistry. 1990; 29:1661–1668. [PubMed: 2159343]
28. Hildebrandt P, Vanhecke F, Buse G, Soulimane T, Mauk A. G Resonance Raman Study of the Interactions between Cytochrome c Variants and Cytochrome c Oxidase. Biochemistry. 1993; 32:10912–10922. [PubMed: 8399241]
29. Robinson NC, Neumann J, Wiginton D. Influence of detergent polar and apolar structure upon the temperature dependence of beef heart cytochrome *c* oxidase activity. Biochemistry. 1985; 24:6298–6304. [PubMed: 3002436]

30. Soulimane T, Buse G. Integral cytochrome-*c* oxidase. Preparation and progress towards a three-dimensional crystallization. Eur. J. Biochem. 1995; 227:588–595. [PubMed: 7851442]
31. Fabian M, Palmer G. Hydrogen peroxide is not released following reaction of cyanide with several catalytically important derivatives of cytochrome c oxidase. FEBS Lett. 1998; 422:1–4. [PubMed: 9475157]
32. Baker GM, Noguchi M, Palmer G. The Reaction of Cytochrome Oxidase with Cyanide. J. Biol. Chem. 1987; 262:59544.
33. Sedlák E, Robinson NC. Phospholipase A(2) digestion of cardiolipin bound to bovine cytochrome *c* oxidase alters both activity and quaternary structure. Biochemistry. 1999; 38:14966–14972. [PubMed: 10555978]
34. Margoliash E, Frohwirt N. Spectrum of horse-heart cytochrome *c*. Biochem J. 1959; 71:570–572. [PubMed: 13638266]
35. Bergmayer, HU.; Gawehn, K.; Grassl, M. Enzymes as Biochemical Reagents in Methods of Enzymatic Analysis. In: Bergmayer, HU., editor. Engl. Transl. Vol. Vol. 1. Weinheim: Verlag Chemie; 1974. p. 425
36. Fabian M, Palmer G. The interaction of cytochrome oxidase with hydrogen peroxide: the relationship of compound P and compound F. Biochemistry. 1995; 34:13802–13810. [PubMed: 7577973]
37. Wikstrom M, Morgan JE. The dioxygen cycle. Spectral, kinetic, and thermodynamic characteristics of ferryl and peroxy intermediates observed by reversal of the cytochrome oxidase reaction. J. Biol. Chem. 1992; 267:10266–10273. [PubMed: 1316895]
38. Liu Y-C, Sowdal LH, Robinson NC. Separation and quantification of cytochrome c oxidase subunits by Mono-Q fast protein liquid chromatography and C18 reverse-phase high performance liquid chromatography. Arch. Biochem. Biophys. 1995; 324:135–142. [PubMed: 7503548]
39. Bligh EG, Dyer WJ. A rapid method of total lipid extraction and purification. Can. J. Biochem. Physiol. 1959; 37:911–917. [PubMed: 13671378]
40. McDonald-Marsh T, Carroll CA, Robinson NC, Musatov A. Matrix-assisted laser desorption/ionization time-of-flight mass spectrometry analysis of cardiolipin extracted from detergent-solubilized mitochondrial electron transfer complexes. Anal. Biochem. 2006; 359:262–263. [PubMed: 17049476]
41. Buege JA, Aust SD. Microsomal lipid peroxidation. Methods Enzymol. 1978; 52:302–310. [PubMed: 672633]
42. Palmer G. Electron paramagnetic resonance. Methods Enzymol. 1967; 10:594–609.
43. Nourooz-Zadeh J. Ferrous ion oxidation in presence of xylenol orange for detection of lipid hydroperoxides in plasma. Methods Enzymol. 1999; 300:58–62. [PubMed: 9919509]
44. Schejter A, George P. The 695-nm band of ferricytochrome and its relationship to protein conformation. Biochemistry. 1964; 3:1045–1049. [PubMed: 14220663]
45. George P, Tsou CL. Reaction between hydrocyanic acid, cyanide ion and ferricytochrome c. Biochem. J. 1952; 50:440–448. [PubMed: 14925115]
46. Varhač R, Tomášková N, Fabián M, Sedlák E. Kinetics of cyanide binding as a probe of local stability/flexibility of cytochrome c. Biophys. Chem. 2009; 144:21–26. [PubMed: 19545938]
47. Varhač R, Antalík M. Correlation of acid-induced conformational transition of ferricytochrome c with cyanide binding kinetics. J. Bio. Inorg. Chem. 2008; 13:713–721. [PubMed: 18317818]
48. Bren KL, Gray HB, Banci L, Bertini I, Turano P. Paramagnetic ^{1}H NMR spectroscopy of the cyanide derivative of Met80Ala-iso-1-cytochrome *c*. J. Am. Chem. Soc. 1995; 117:8067–8073.
49. Schejter A, Aviram I. The reaction of cytochrome c with imidazole. Biochemistry. 1969; 8:149–153. [PubMed: 5777317]
50. Sutin N, Yandell JK. Mechanisms of the reaction of cytochrome c. J. Biol. Chem. 1972; 247:6932–6936. [PubMed: 4343163]
51. Barr DP, Mason RP. Mechanism of radical production from the reaction of cytochrome c with organic hydroperoxides. J. Biol. Chem. 1995; 270:12709–12716. [PubMed: 7759524]

52. Cheng G, Wysocki VH, Cusanovich MA. Local stability of *Rhodobacter capsulatus* cytochrome c_2 probed by solution phase hydrogen/deuterium exchange and mass spectrometry. J. Am. Soc. Mass. Spectrom. 2006; 17:1518–1525. [PubMed: 16872833]
53. Brittain T, Baker AR, Butler CS, Little RH, Lowe DJ, Greenwood C, Watmough NJ. Reaction of variant sperm-whale myoglobins with hydrogen peroxide: the effects of mutating a histidine residue in the haem distal pocket. Biochem. J. 1997; 326:109–115. [PubMed: 9337857]
54. Davies MJ. Identification of a globin free radical in equine myoglobin treated with peroxides. Biochim. Biophys. Acta. 1991; 1077:86–90. [PubMed: 1849014]
55. Schlichting I, Berendzen J, Chu K, Stock AM, Maves SA, Benson DE, Sweet RM, Ringe D, Petsko GA, Sligar SG. The catalytic pathway of cytochrome P450cam at atomic resolution. Science. 287:1615–1622. [PubMed: 10698731]
56. Hamachi I, Fujita A, Kunitake T. Enhanced N-demethylase activity of cytochrome c bound to a phosphate-bearing synthetic bilayer membrane. J. Am. Chem. Soc. 1994; 116:8811–8812.
57. Rosei MA, Blarzino C, Coccia R, Foppoli C, Mosca L, Cini C. Production of melanin pigments by cytochrome c/H_2O_2 system. Int. J. Biochem. Cell. Biol. 1998; 30:457–463. [PubMed: 9675879]
58. Diederix RE, Ubbink M, Canters GW. The peroxidase activity of cytochrome c-550 from Paracoccus versutus. Eur. J. Biochem. 2001; 268:4207–4216. [PubMed: 11488914]
59. Hackenbrock CR, Chazotte B, Gupte SS. The random collision model and a critical assessment of diffusion and collision in mitochondrial electron transport. J. Bioenerg. Biomembr. 1986; 18:331–368. [PubMed: 3021714]
60. Belikova NA, Vladimirov YA, Osipov AN, Kapralov AA, Tyurin VA, Potapovich MV, Basova LV, Peterson J, Kurnikov IV, Kagan VE. Peroxidase activity and structural transition of cytochrome c bound to cardiolipin-containing membranes. Biochemistry. 2006; 45:4998–5009. [PubMed: 16605268]
61. Mansouri A, Muller FL, Liu Y, Ng R, Faulkner J, Hamilton M, Richardson A, Huang T-T, Epstein CJ, Remmen H. Alterations in mitochondrial function, hydrogen peroxide release and oxidative damage in mouse hind-limb skeletal muscle during aging. Mech. Ageing. Dev. 2006; 127:298–306. [PubMed: 16405961]
62. Nulton-Persson AC, Szweda LI. Modulation of mitochondrial function by hydrogen peroxide. J. Biol. Chem. 2001; 276:23357–23361. [PubMed: 11283020]

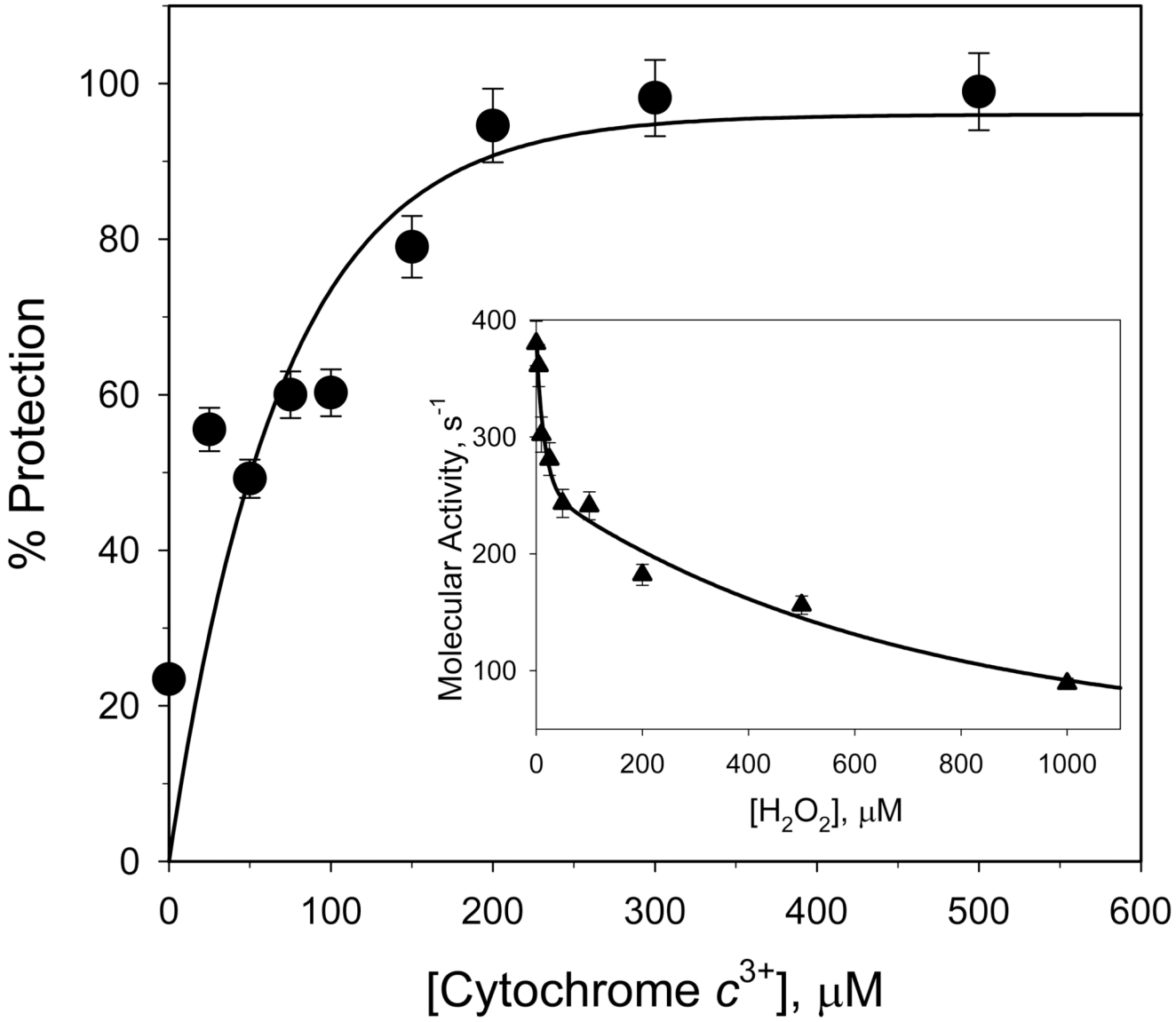

Figure 1. Ferricytochrome c protection of CcO from inactivation by H_2O_2

Main panel: Electron transfer activity of CcO after its exposure to H_2O_2 in the presence of different concentrations of cyt c^{3+}. Cytochrome *c* oxidase (10 μM) was reacted with 500 μM H_2O_2 for 30 min in the presence of 0–500 μM ferricytochrome *c*. The reaction was stopped by removal of H_2O_2 using anion-exchange chromatography, and the remaining CcO activity determined spectrophotometrically. Data were fitted to a single-exponential rise to a maximum (solid line). Inset panel: Inactivation of CcO by H_2O_2 in the absence of cyt c^{3+}. Cytochrome *c* oxidase (10 μM) was reacted with each concentration of H_2O_2 for 30 min., excess H_2O_2 removed by anion-exchange chromatography, and the remaining CcO activity determined spectrophotometrically. Data were fitted to a single-exponential decay (solid line). Assays were performed in triplicate using three different CcO preparations. The standard deviation in experiments was estimated to be ± 5.0%.

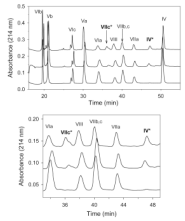

Figure 2. Cytochrome c oxidase nuclear-encoded subunit composition after exposure to H_2O_2 in the presence or absence of ferricytochrome c

Cytochrome *c* oxidase (10 μM) was reacted with 500 μM H_2O_2 in the presence of either 0, 300, or 500 μM cyt c^{3+} (top, middle and lower chromatograms). After 30 min., H_2O_2 and cyt c^{3+} were removed by HiTrap Q anion exchange chromatography and the nuclear-encoded subunit composition quantified by RP-HPLC analysis of 0.5 nmol of CcO [27]. Upper panel: RP-HPLC elution profile for all 10 of the nuclear-encoded subunits. Lower panel: Expanded profile between 33 to 49 min to better illustrate the elution of the H_2O_2 modified subunits (IV* and VIIc*). The data represents typical RP-HPLC profiles of three experiments using three different CcO preparations.

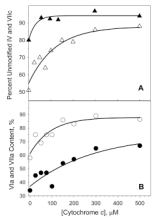

Figure 3. Ferricytochrome c protection of CcO subunits from H_2O_2-induced modifications

Panel A: Protection of CcO subunits IV (filled triangles) and VIIc (open triangles) from H_2O_2-induced oxidations by increasing cyt c^{3+} concentration. Panel B: Protection of CcO subunits VIa (filled circles), and VIIa (open circles) from H_2O_2-induced dissociation by increasing cyt c^{3+} concentration. The percent modification of each subunit was calculated from the areas of the relevant RP-HPLC elution peaks. Differences between chromatograms were normalized on the assumption that the area under the RP-HPLC peak corresponding to subunit Va remained constant. Solid lines are single-exponential fits to the data. The results are presented as an average of three measurements using three different preparations of CcO. The deviation in experiments was estimated to be ± 4.4%.

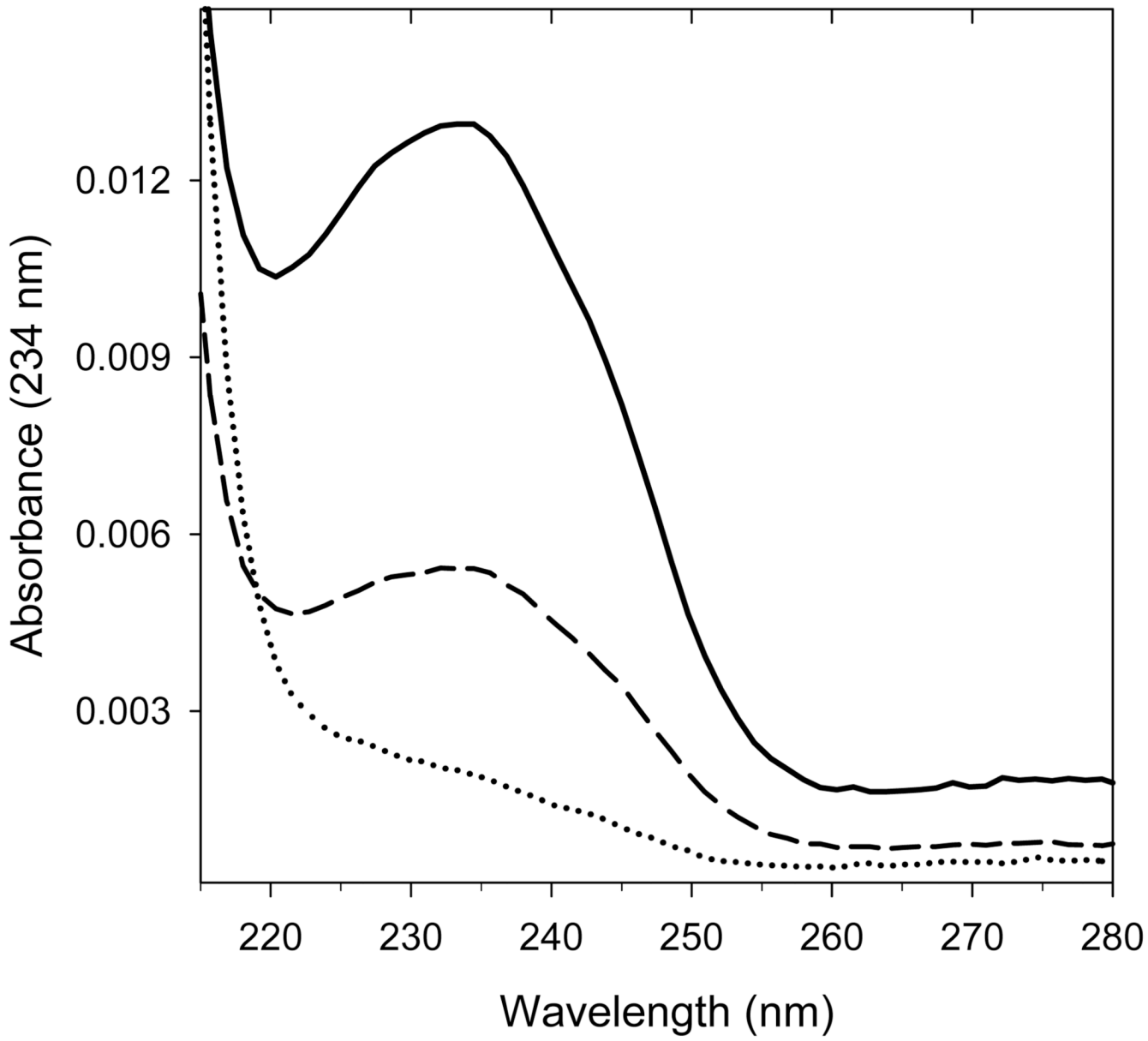

Figure 4. Excess cyt c^{3+} protects CcO-bound cardiolipin from H_2O_2-induced peroxidation

Peroxidized cardiolipin has a characteristic absorbance maximum at 234nm due to the presence of conjugated dienes; therefore, the extent of peroxidation can be determined from the UV spectrum of cardiolipin. The UV spectrum of HPLC-purified CL before (dotted line) and after exposure of CcO to 500 μM H_2O_2 in either the presence (dashed line), or absence (thick solid line) of excess cyt c^{3+}. The UV spectrum was acquired online using a diode-array UV HPLC detector. In each case, cardiolipin was extracted from 2 nmole of CcO, dissolved in ethanol, and purified by HPLC. Nearly identical results were obtained for three different CcO preparations.

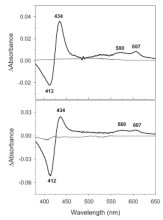

Figure 5. Generation of the H_2O_2-induced CcO oxy-intermediates is unaffected by the presence of excess cyt c^{3+}

CcO **P**- and **F**-oxy-intermediates have a characteristic $CcO_{P+F} - CcO_{oxid}$ difference spectrum with a minimum at 412 nm and maxima at 434, 580 and 607 nm. The difference spectrum for CcO was generated *in silico* by subtracting the digitized visible spectrum of 1.2 μM oxidized CcO in 20 mM Tris-Cl buffer, pH 7.4, with 2 mM dodecyl maltoside, from the digitized spectrum acquired after its reaction with 500 μM H_2O_2 for 30 min in absence and presence of cyt c^{3+}. Upper Panel: H_2O_2-induced difference spectrum of CcO acquired in the absence of ferricytochrome c. Lower Panel: H_2O_2-induced difference spectral changes of cytochrome *c* oxidase in presence of 8 μM ferricytochrome *c*. In this case, the spectrum of ferricytochrome *c* was recorded, set to zero and was used as a reference (thin line). CcO was then added to make the solution 1.2 μM in CcO and the difference spectrum generated as described above. Concentrations of **P**- and **F**- forms were calculated using $\Delta\Delta\varepsilon_{607-630} = 11$ $mM^{-1}cm^{-1}$ for the **P**-form, and $\Delta\Delta\varepsilon_{580-630} = 5.3$ $mM^{-1}cm^{-1}$ for the **F**-form [32]. In both A and B forms of CcO hydrogen peroxide produces essentially the same amount of intermediates.

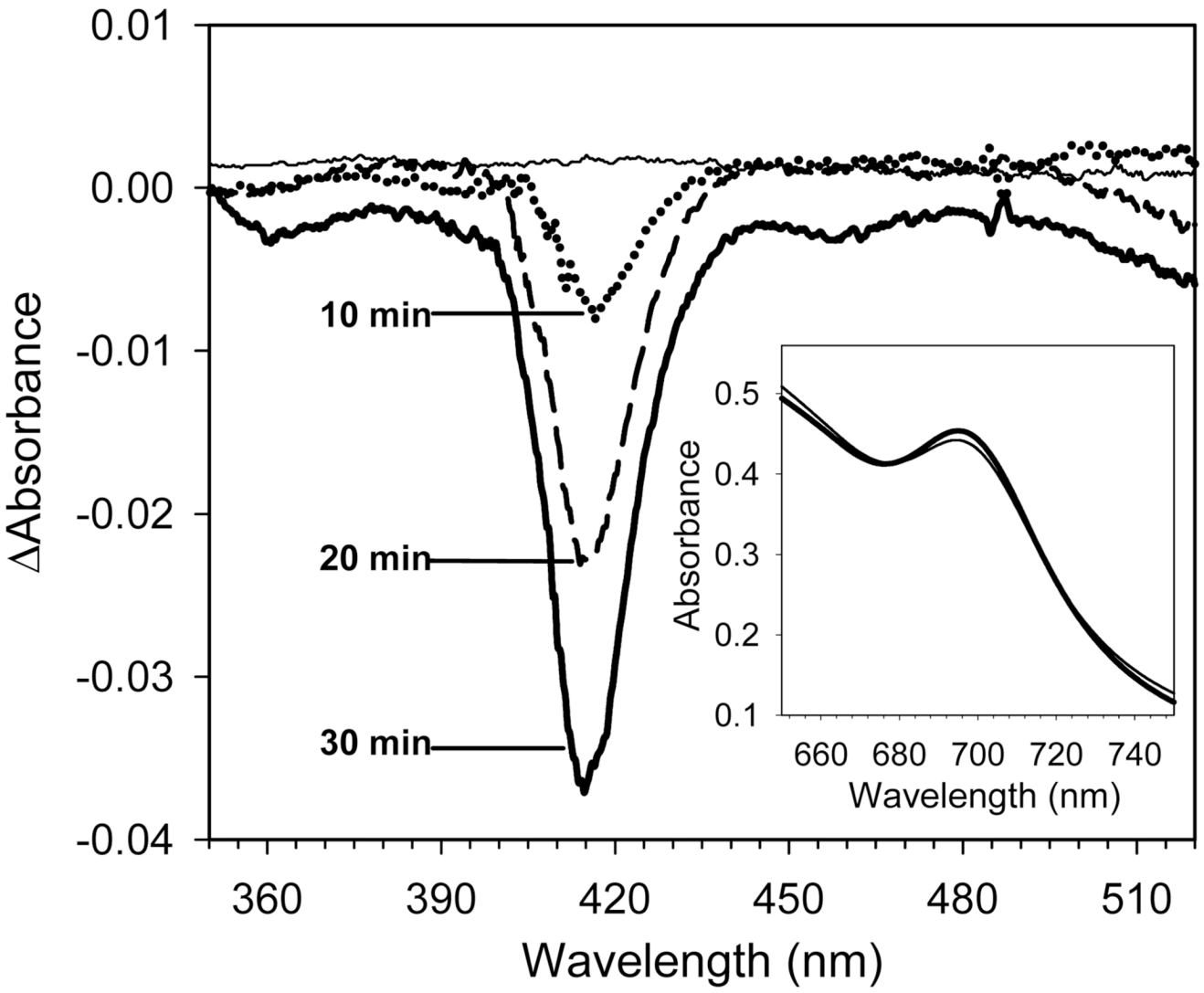

Figure 6. H_2O_2-induced bleaching of the visible spectrum of cyt c^{3+}

Main Panel: Time-dependence of H_2O_2 –induced changes in the Soret difference spectrum of ferricytochrome *c*. Ferricytochrome *c* (500 μM) in 20 mM Tris-Cl pH 7.4 buffer containing 2 mM dodecyl maltoside was reacted with 500 μM H_2O_2 at room temperature. After 0, 10, 20 and 30 min, 10 μL aliquots were diluted 100-fold with reaction buffer and the absolute spectra were recorded. The absorption maxima in absolute spectra were 0.530, 0.527, 0.512, and 0.502, respectively. The difference spectrum was generated by subtracting the digitized visible spectrum of cyt c^{3+} before addition of H_2O_2 from the digitized spectrum acquired after its reaction with H_2O_2. Maximum absorbance in the Soret region decreased by only 0.6%, 3.5%, and 5.3% after 10, 20 and 30 min reaction of cyt c^{3+} with H_2O_2, dotted, dashed, and solid line, respectively.

Inset Panel: H_2O_2-induced changes in the far visible spectrum of a mixture of cyt c^{3+} and CcO. Difference spectra were recorded for 500 μM cyt c^{3+} and 10 μM CcO versus 10 μM CcO before (thick line) and after 30 min reaction with 500 μM H_2O_2 (thin line). Measurements were done in triplicate with the nearly identical results.

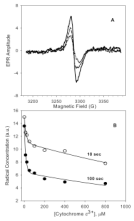

Figure 7. Ferricytochrome c suppression of the H_2O_2-induced free radical EPR signal of CcO

Upper Panel: Difference EPR spectra for CcO in either the absence (solid line), or presence of 100 μM (dashed line), or 800 μM f cyt c^{3+} (dotted line). All samples were frozen within 10 seconds after addition of 500 μM H_2O_2. Each difference spectrum was calculated by subtracting the oxidized CcO spectrum from that of the H_2O_2 treated enzyme. Lower Panel: Dependence of the CcO radical yield upon the cyt c^{3+} concentration for samples reacted with H_2O_2 for either 10, or 100 seconds. Solid lines through each set of data are non-linear regression fits of the data to a two-term exponential decay. The reaction was initiated by addition of 500 μM H_2O_2 to 48.3 μM CcO solubilized in 20 mM Tris-Cl buffer, pH 7.4, containing 2 mM dodecyl maltoside and 4 mM K_2SO_4. Refer to *Experimental Procedures* for EPR experimental details. The results are presented as an average of three experiments employing two different preparations of CcO.

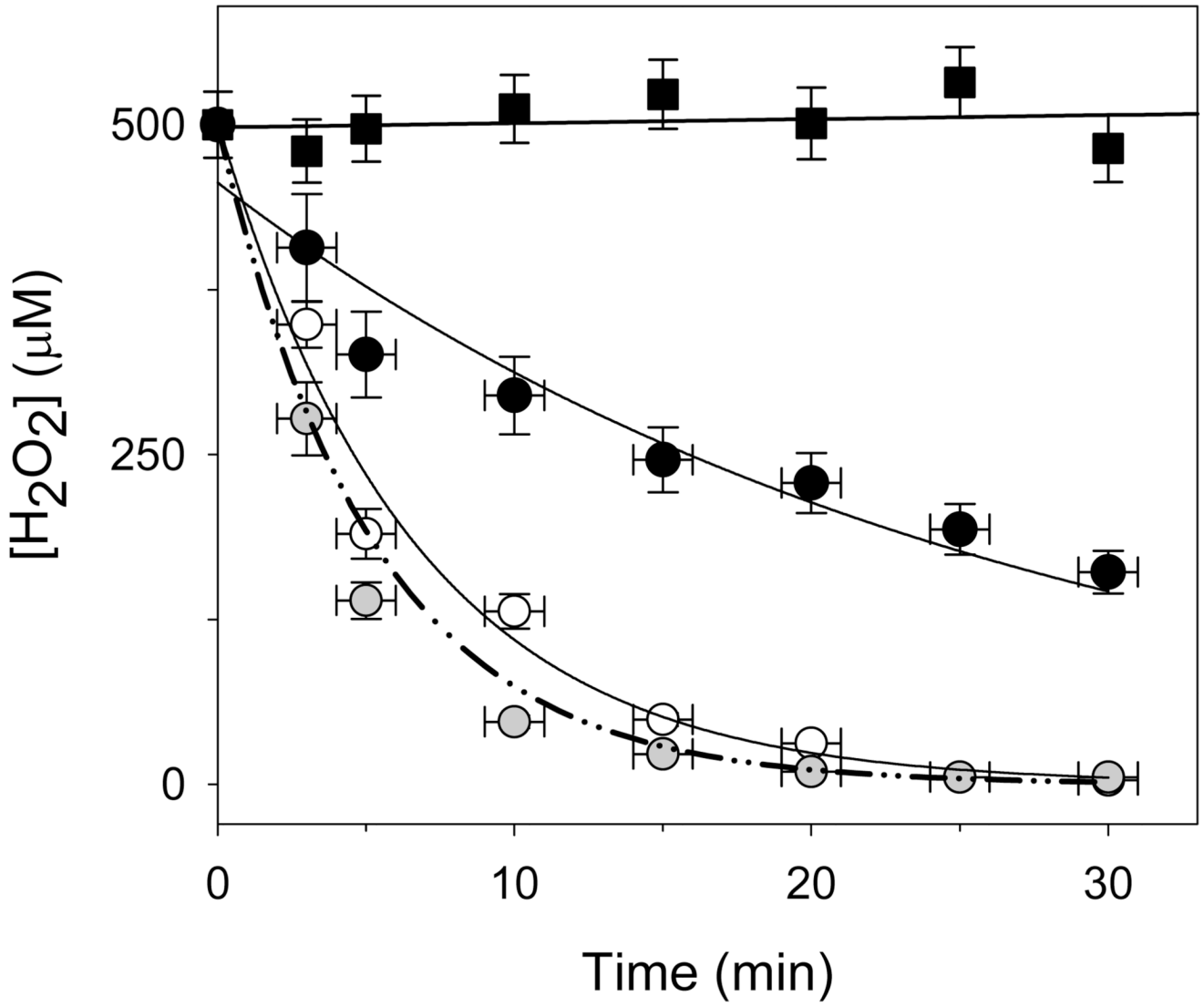

Figure 8. Decomposition of H_2O_2 by cyt c^{3+}, CcO, and a mixture of cyt c and CcO

The peroxidase activity of 500 μM cyt c^{3+} (unfilled circles), 500 μM cyt c^{3+} that previously had been reacted with 10 mM KCN for 1 hour at RT (black-filled squares), 10 μM CcO (black-filled circles), and a mixture of 500 μM *cyt* c^{3+} and 10 μM CcO (grey-filled circles) were quantified by following the destruction of 500 μM H_2O_2 as a function of time using the FOX2 assay. The solid lines are non-linear regression fits of the cyt c^{3+} and CcO data to single exponentials, with second order rate constants of 5.1 $M^{-1}s^{-1}$ and 63.2 $M^{-1}s^{-1}$, respectively (the rate constant for KCN reacted cyt c^{3+} was essentially zero). The dot-dash line is the theoretical first order rate for a mixture of 500 μM cyt c^{3+} and 10 μM CcO using the two second order rate constants. All reactions were done in 20 mM Tris-Cl, pH 7.2 buffer, containing 2 mM dodecyl maltoside. The provided data are mean values of three independent experiments using three different CcO preparations and the error bars correspond to standard deviations of the measurements.